URN (Paper): urn:nbn:de:gbv:ilm1-2014iwk-175:8

58th ILMENAU SCIENTIFIC COLLOQUIUM
Technische Universität Ilmenau, 08 – 12 September
2014 URN: urn:nbn:de:gbv:ilm1-2014iwk:3

TECHNICAL, NON-VISUAL CHARACTERIZATION OF SUBSTRATE CONTACT USING CARPAL VIBRISSAE AS A BIOLOGICAL MODEL: AN OVERVIEW

Schmidt, M.[1]; Witte, H.[2]; Zimmermann, K.[3];
*Niederschuh, S.[1]; **Helbig, T.**[2]; Voges, D.[2]; Husung, I.[3]; Volkova, T.[3]; Will, Ch.[3];*
Behn, C.[3]; Steigenberger, J.[4]; Klauer, G.[5]

[1] Institut für Spezielle Zoologie und Evolutionsbiologie mit Phyletischem Museum, Friedrich-Schiller-Universität Jena, Germany · [2] Chair of Biomechatronics, Faculty of Mechanical Engineering, Technische Universität Ilmenau, Germany · [3] Chair of Technical Mechanics, Faculty of Mechanical Engineering, Technische Universität Ilmenau, Germany · [4] Institute of Mathematics, Technische Universität Ilmenau, Germany · [5] Fachbereich der Medizin Johann-Wofgang-von-Goethe-Universität Frankfurt, Dr. Senckenbergische Anatomie und Carolinum, Germany

Abstract. During the flow of evolution, animals have developed specific sensory systems for the interaction with their environment. One example are tactile hairs – so called sinus hairs or vibrissae – on the body surfaces of mammals. These sinus hairs provide inspiration for technical development, since the variability of the biological sensors is due to mechanical structure. The aim of our research is to provide a technical, non-visual characterization of substrate contacts based on the biological model of carpal sinus hairs of rats. Rats live in a tactile world, they have poor visual acuity and lack binocular fusion, making their tactile senses crucial in very different occasions, regarding orientation, locomotion, grasping and more. Carpal sinus hairs may be found at the distal end of the lower arm near the carpal bones in arboreal mammals as well as in mammals with high grasping abilities.

In this contribution, we present methods and first results from motion studies with living rats are introduced, which shall help to clarify the functionality and role of carpal sinus hairs in the detection of substrate disturbances, which investigate the influence of mystacial and carpal sinus hairs on different walking parameters, analyses of geometrical, structural and mechanical properties of carpal sinus hairs and the transfer of these into mechanical models, and at last a macroscopic model of a sinus hair.

Mathematico-mechanical models at various levels of abstraction (rigid body models, continuum mechanics), based on experiments (movement studies, biomechanical measurements), and analyses of the results serve as an augmentation in basic research as well as a foundation for biomimetic (more exactly: bionic) transfer.

Index Terms – sinus hair · vibrissae · carpal · tactile sensor · substrate contact · non-visual · statics and dynamics · applied mechanics

1. INTRODUCTION

Vibrissae or sinus hairs are known from, e.g., rats, cats, seals or hamsters. These animals use different habitats, are competent climbers or swimmers, or possess high grasping skills. Olfactory and visual senses help to coordinate positional control of the locomotion during the above mentioned activities, but this may not be sufficient, if animals hunt in dark environment [13, 14, 16, 39, 43]. The senses of touch are very important abilities not only implying social factors, but grasping activities and determination of surface conditions as well as establishing a role in body stabilization. Within the stem lineage of *Theria* a reorganization of limbs and vertebrae took place which resulted in a high dynamic stability during locomotion on discontinuous substrate [10]. To support such a balanced motion of the trunk, special sensors were added. One of these sensors are the sinus hairs, which have a high sensibility for surface contact and might assist the limbs during a stabilized walking over different substrates [12, 17, 40].

For object determination and texture discrimination, mammals especially use mystacial vibrissae as high-acuity sensors. During a typical foveal whisking, animals thrust their mystacial vibrissae forward to sweep against and over an object ahead of them. Rats, for example, can differentiate rough and smooth surfaces with a groove depth of 30 µm [8]. The ability of mammals to make these high-acuity distinctions prompts that the vibrissa system is made for acquisition of information with high-frequency. The vibrissa, namely, a thin, long, pliable hair attached underneath the skin in a follicle-sinus complex, has no receptors along its length [9]. Therefore, all the tactile signals at the tip of the vibrissa must be transmitted mechanically to sensory receptors inside the follicle-sinus complex (Fig. 1). According to HARTMANN et al. [20] and NEIMARK et al. [30] mechanical resonance properties of vibrissae could facilitate detection, and bandpass filter properties may enhance texture discrimination. The vibration of vibrissae with emphasis on prediction of natural resonant frequencies was investigated theoretically by YAN et al. [46].

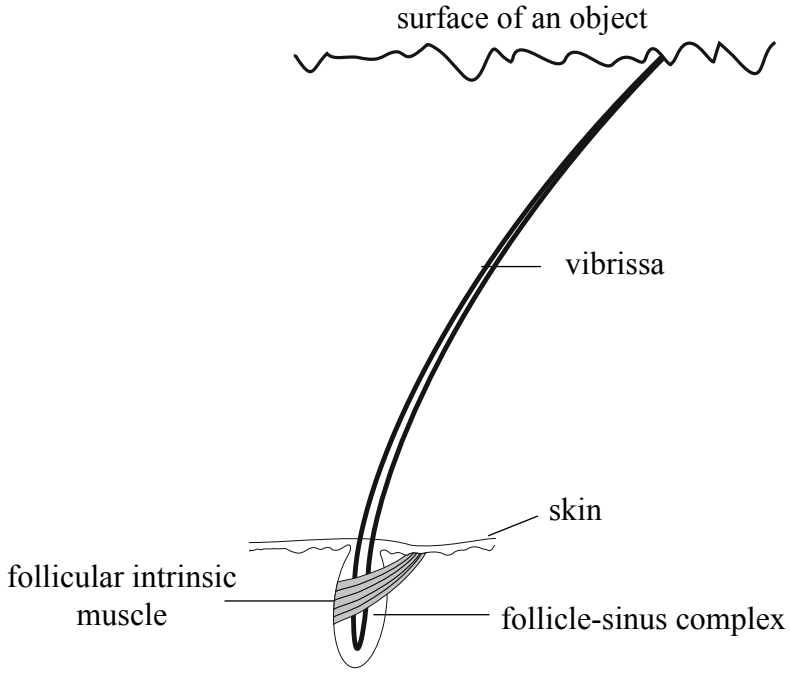

Fig. 1: Schematic drawing of a vibrissa sweeping past a rough surface

2. CATEGORIZATION OF HAIRS

All mammals except humans reveal three different types of hairs, so called vellus hair, guard hairs and sinus hairs [43]. Human skin lacks sinus hairs. In mammalian hairy skin all sinus and guard hairs, and many vellus hairs, are tactile organs. They reveal differences in innervation amount and types of mechanoreceptors [11], [18]. In this section, hairs shall be differentiated regarding their innervation and sensory features to gain insight on their sensory capabilities (Fig. 2).

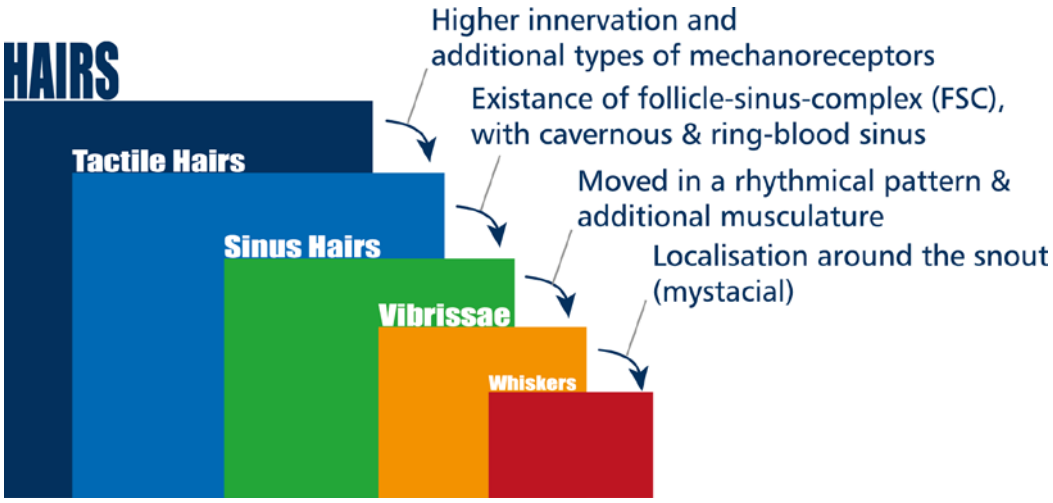

Fig. 2: Classifiction of specialized tactile hairs of mammals regarding innervation and other sensory features

Least innervated are *vellus hairs* (lanugo or pelage hair). They mostly possess only some free nerve endings (nociceptors). Just larger vellus hairs feature free and lanceolate nerve endings (velocity receptors). Merkel nerve endings (pressure receptors) at vellus hairs appear only in some few body regions. Other nerve endings are very uncommon. *Guard hairs* (tylotrich hair or contour hair) in comparison feature more nerve endings. They have more free nerve endings, up to 20 Merkel cell nerve endings and lanceolate nerve endings each, and pilo-Ruffini corpuscles (tension receptors) at each hair follicle [18].

Sinus hairs are a special characteristic of *Theria* [27, 29, 32, 34, 35]. These sensors own a follicle-sinus-complex, which surrounds the normal root of the hair: the hair follicle is almost completely embedded in a blood sinus and in large follicles equipped with more than 2.000 sensory nerve endings [11, 19]. The types of nerve endings and receptors are comparable to that of guard hairs, although their number is way bigger. Instead of 20 Merkel nerve endings they have some 500 to 2.000. Additionally, lamellated corpuscels of Pacini type (acceleration detectors) can be found in each follicle [18]. Furthermore, sensory nerve endings show a constant topographic pattern [19, 37].

Vibrissae (Latin, singular *vibrissa)* are sinus hairs, which move in a rhythmic pattern. Recent studies have even shown that rats actively change the patterns of their mystacial vibrissae according to different boundary conditions [2]. The common term '*whiskers*' has to be used with special attention. Colloquially 'whiskers' means a summarization of mystacial sinus hairs of all mammals, independent of their rhythmic moving ability. 'Whisking' is a rhythmic movement of the sinus hairs. For this reason, whiskers can be interpreted as a subgroup of vibrissae, which are specially located (Fig. 2), or as a direct subgroup of sinus hairs parallel to vibrissae.

3. AIMS OF THE STUDY PRESENTED

The main focuses of the overall investigation are:

- clarification of the role of carpal sinus hairs on the detection of substrate disturbances,
- analysis of geometrical, structural and mechanical properties of carpal sinus hairs from *Rattus norvegicus* by microscopy (light microscopy, SEM), µCT and via force/displacement measurements,
- modeling and computer-based simulation carpal sinus hairs, based on models with different degree of abstraction (multi-body systems with low degree of freedom to continuum models) and dynamics.

For these purposes, a better understanding of the mechanical behaviour of sinusoidal hairs as well has to include aspects concerning mystacial as well as carpal sinus hairs:

- simulation of the contact process of the sinus hairs using analytical and numerical methods as well as
- development, implementation and simulation of control algorithms for the reproduction of the sensual capacity in sinus hairs sensory systems.

In the current study, methods and results are introduced, which shall help to clarify the functionality and role of carpal sinus hairs. Therefore, motion studies with living rats, which examine the influence of mystacial and carpal sinus hairs on different walking parameters as well as analyses of geometrical, structural and mechanical properties of carpal sinus hairs, are performed. Integrating these results with information available from literature, the process of foveal whisking based on the mechanical model of the vibrissa as an EULER-BERNOULLI beam is investigated theoretically. Conditions of parametric resonance are obtained, when the vibrissa performs oscillations, whose amplitude progressively increases.

4. CARPAL SINUS HAIRS

Sinus hairs can be found on different body parts and are named after their position [26, 41].

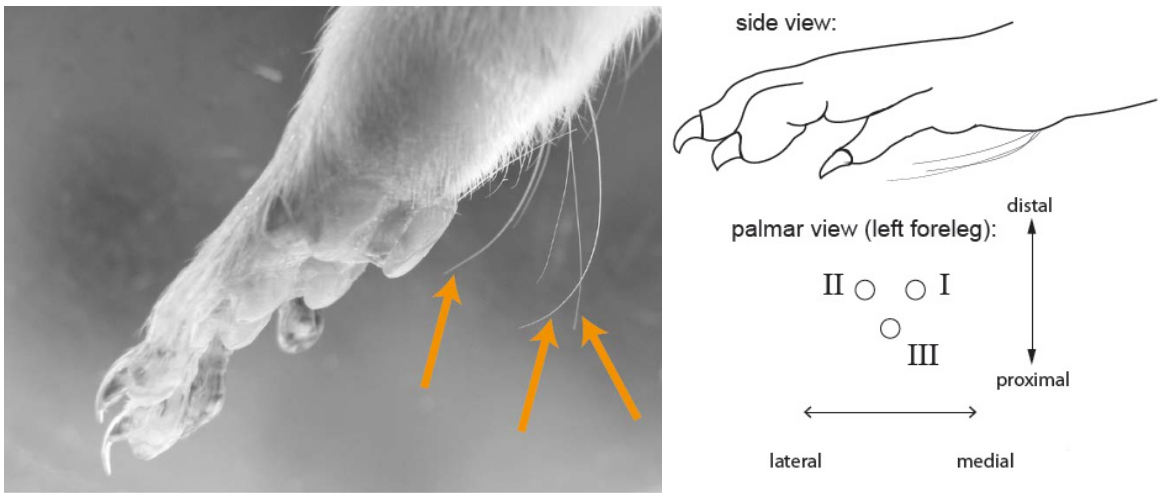

Fig. 3: Triple of carpal vibrissae (arrows) at a forelimb of *Rattus norvegicus* right – schematic illustration with positional relations and numbering

Carpal sinus hairs can be found at the distal end of the lower arm close to the carpal bones in arboreal species as well as in species with a high grasping ability [3, 29, 41], e.g., *Galidia elegans, Herpestes ichneumon, Martes martes, Mustela nivalis, Cricetus cricetus, Meriones persicus, Ondatra zibethicus, Sigmodon hispidus, Xerus inauris*. While the knowledge about carpal sinus hairs in comparison to especially mystacial sinus hairs is very limited, this study deals with carpal sinus hairs of *Rattus norvegicus*. Carpal sinus hairs of rats appear in a number of about three (Fig. 3).

4.1 Follicle-Sinus-Complex

General Structure

In general, the follicle-sinus-complex of carpal sinus hairs is comparable to that of mystacial sinus hairs. They possess a follicle-sinus-complex with a cavernous and a ring sinus, sebaceous glands, relative thick septum around the follicle and collagenous capsule as well as a high innervation with different types of mechanoreceptors [11, 25]. But FUNDIN et al. [11] have shown differences in type and number of mechanoreceptors between mystacial and carpal sinus hairs.

Furthermore, observations often show the existence of two hairs in one follicle, which are separated through own cellular rings. We assume that it is a matter of coexistence of an old and a renewable hair.

Innervation

A comparative study of FUNDIN et al. [11] between differently located sinus hairs reports differences in innervation as well as in number and types of mechanoreceptors between carpal and mystacial sinus hairs [36, 38]. Functional differences between sinus hairs in different locations seem obvious. Among the types investigated carpal sinus hairs show the most pronounced deviations from the typical follicle-sinus-pattern of innervation. The innervation of the inner conical body (ICB) is relatively sparse in comparison to mystacial follicle-sinus-complexes. No circumferentially oriented nerve endings are connected to the ICB. Furthermore, a large section of the carpal ICB innervation ascends from the deep vibrissal nerve, which is rarely seen in other follicle-sinus-complexes.

Carpal sinus hairs feature relatively few ring-sinus Merkel endings, which are diffusely distributed. They lack reticular and irregular lanceolate-like endings in the cavernous sinus and have extremely few lanceolate endings in comparison to other sinus hairs. Instead they show a unique set of corpuscular endings (afferents that terminated in bulb-like swellings) in the ICB, ring sinus and cavernous sinus, which are placed distant from the glassy membrane. Fundin et al. assume that they are corpuscular endings with multiple lamellae (in comparison to ANDRES [1]), but no replacement for reticular endings. Some carpal sinus hairs were examined that are innervated by cervical dorsal root ganglion cells. These did not contain any lanceolate endings.

With the sparse Merkel innervation, it has to be assumed that carpal sinus hair are less precise regarding directional sensitivity than other sinus hairs. Merkel endings are purported to have a high directional sensitivity [15].

Musculature

Own histological observations show that strong muscles are connected with the capsule of carpal sinus hairs in the lower third. This suits studies made by FUNDIN et al. [11] who found a sling-like piloerector muscle affiliated to the follicle-sinus-complex. This muscle is attached to the skin at the side where the sinus hair shaft forms an acute angle with the skin. With this muscle, follicle-sinus-complex and hair can be levered to a more perpendicular or opposite position.

Carpal sinus hairs have not been observed so far to be moved in a rhythmic pattern or to change strategy in vibrissal active sensing like mystacial sinus hairs [2]. Lacking this information at present, it has to be assumed that carpal sinus hairs cannot be moved rhythmically to support sensing function. So they might play a role model for passive, but not for actively moved sensor systems.

4.2 Hair

After different studies on length, diameter, weight, Young's modules and other mechanical parameters regarding mystacial sinus hairs [6, 7, 33, 44], some of our current studies collect comparable data for carpal sinus hairs. Due to the smaller size of carpal sinus hairs, methods used for mystacial sinus hairs have to be adapted or new approaches have to be found. Differences or similarities between carpal and mystacial sinus hairs might point on crucial parameters for sensor functionality and biological role.

For all carpal sinus hairs, examinations are based on 20 female and 20 male rats to ensure a statistical relevant amount of probes. Statistical data later on will be used as parameters for mechanical models (see chapter 5) and macroscopic demonstrators (see chapter 6).

Geometric Parameters

Analyses of geometric parameters of carpal sinus hair are based on macrophotography (length and curvature) and light microscopy (diameter). For macrophotography a Canon® 60D with a Canon® 100 mm 1:2.8L IS USM lens was used, allowing to take a picture of a complete sinus hair, and to preserve natural curvature of the hair. With this setup, a spatial resolution of 4,3 µm can be achieved at a magnification of 1:1. Light microscopy is done with an Olympus® BX 51 system microscope with a magnification of 20 x (Fig. 4) and 40 x (Fig. 5, right). Single pictures are stitched automatically using the data from the x-y-coordinate table. Stitching of microscopic pictures taken with a Canon®60D mounted to a Carl Zeiss® AxioStar Plus microscope without automated x-y-coordinate table failed due to too small changes in diameter of the sinus hair along the length.

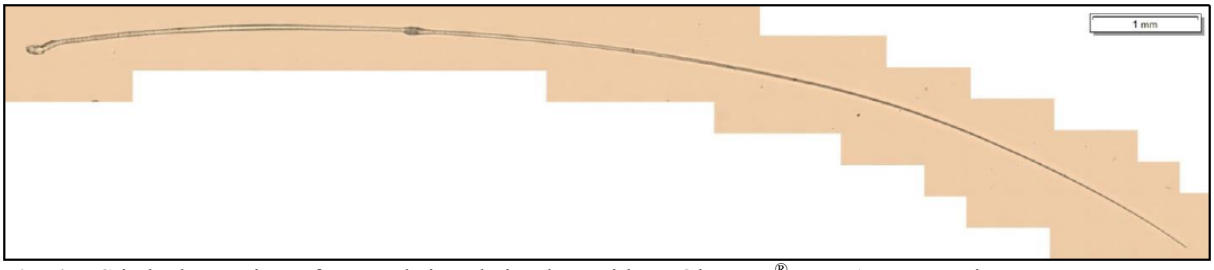

Fig. 4: Stitched overview of a carpal sinus hair taken with an Olympus® BX 51 system microscope at a magnification of 20 x

Preliminary tests indicate that length and diameter of carpal sinus hairs are smaller than that of mystacial macro vibrissae [44]. Lengthes shorter than 10 mm and basal diameters (cp. Fig. 5) less than 60 µm have to be expected for carpal sinus hairs. Still methodical problems like determination of basal end/beginning of the follicle have to be solved (Fig. 5, right).

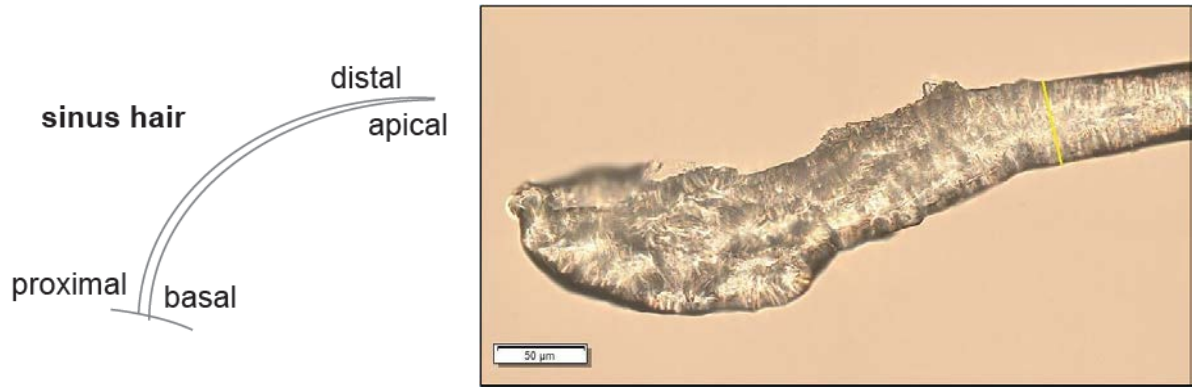

Fig. 5: left – Schematic overview of a sinus hair with relevant relations of position.
right – Detail of the root section of a carpal sinus hair with manually selected basal end of the hair. Picture is taken with an Olympus® BX 51 system microscope at a magnification of 40 x

Inner Structure

To describe the inner structure of carpal sinus hairs by parameters like thickness of cuticula and cortex, existence and distribution of the medulla as well as chemical compounding, different methods are tested (Fig. 6, 7). Scanning electron microscopy (SEM) was performed at iba® (Institute for Bioprocessing and Analytical Measurement Techniques, Bad Heiligenstadt) and at Friedrich-Schiller-Universität Jena (FSU). High-resolution µCT-scans were realized at Max Planck Institute for Evolutionary Anthropology (Leipzig). Laser scanning microscopy was done at FSU and Center of Micro- and Nanotechnologies (ZMN, Ilmenau). Energy dispersive x-ray microscopy (EDX) as well as forced ion beam microscopy (FIB) were done at ZMN. Fluorescence and polarization microscopy were done at laboratories of the Department of Biomechatronics (Ilmenau).

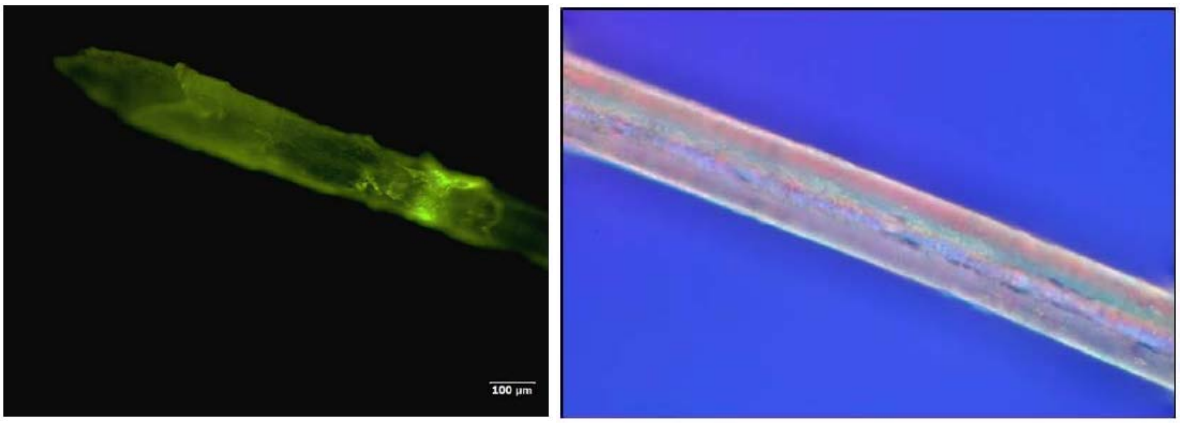

Fig. 6: left – Fluorescence microscopic picture of the basal area of a mystacial sinus hair. Picture is taken with a Carl Zeiss® AxioTech 100HD microscope at a magnification of 10 x.
right – Polarization microscopic picture of the middle section of a carpal sinus hair. Picture is taken with a Carl Zeiss® AxioTech 100HD microscope.

Fig. 7: left – SEM picture of the cuticular area of a carpal sinus hair at a magnification of 10.000 x.
right – EDX mapping of a sliced carpal sinus hair. Distribution of secondary electrons (SE, grey), carbon (C, turquoise) and sulphur (S, red)

Mechanical Parameters

Mechanical parameters like Young's modulus, bending stiffness, Eigen-frequency and damping are obtained by static and dynamic methods. Our aim is to map (especially scale) these properties of carpal sinus hairs by mechanical modeling to mystacial sinus hairs and to compare functionalities.

Static measurements are done with the Basalt Must from Tetra GmbH (Ilmenau), with special regard on the influences of different types of fixation of the single hair (Fig. 8). Bending line and bending stiffness are recorded for different distances to the basal end of the sinus hair. Preliminary tests show a qualitatively similar bending behavior of the carpal sinus hairs in comparison to mystacial sinus hairs. Differentiation to other body hairs can be pointed out clearly.

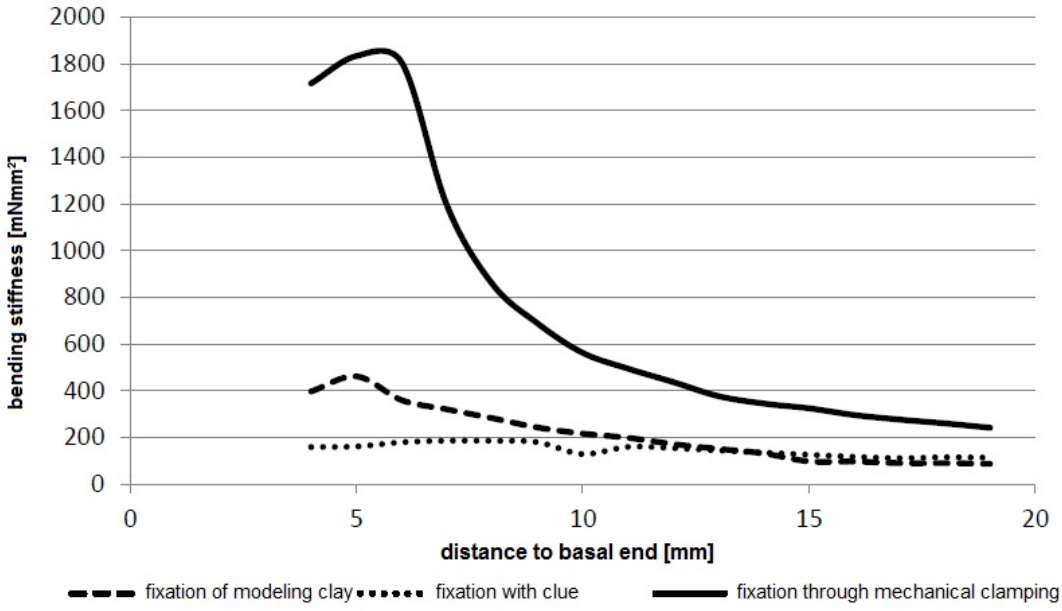

Fig. 8: Comparison of the influence of different fixations on the bending line of a mystacial sinus hair

Dynamic measurements are done in two ways: via a single deflection – different ways to deflect the sinus hair are examined – of a carpal sinus hair, and the analysis of the provoked free oscillation. Alternatively, we analyse forced oscillation with a shaker.

Results of measurements on geometry, structure and mechanical parameters will be published in separate articles.

4.3 Biological role

FUNDIN et al. [11] assume that the effective stimuli of carpal sinus hairs might include behaviour such as eating and grasping, or perhaps might participate in detection of vibrations from the ground. Other hypotheses to the biological role of carpal sinus hairs concentrate on influences on locomotion and the kinematics of the segmental chain of legs.

Mystacial vibrissae detect vertical obstacles and can measure the spatial body position [16, 24]. To recognize obstacles and substrate composition is a very important skill to assure a stabilized body position during locomotion. Touchdown of the forelimbs occurs in a touching gap between the right and left mystacial vibrissae beneath the head. So another sensor has to measure discontinuities of the substrate where touchdown takes place. Carpal sinus hairs are mentioned to recognize irregular substrate and prevent the limbs from stepping into these. This has to be examined precisely to understand the biological role. Carpal sinus hairs exhibit a different length, position and a curved shape. The position of the forelimbs is an important factor for a stabilized locomotion. Carpal sinus hairs might detect intensities of horizontal disturbances and might lead to an adaption of the kinematic walking parameters. But how is that done? First studies suggest a temporal measurement during stance phase, while mystacial vibrissae react with a change of the excursion range [31]. This leads to the hypothesis of a coupling of sinus hair touch and walking sensors on the forelimbs. To test this hypothesis, mystacial vibrissae seem to compensate a loss of the carpal sensors. The swing phase, that is the critical period during limb motion, is characterized by a surface touching of the mystacial vibrissae and, shortly before touchdown, by the contact of the carpal sinus hairs to the substrate. The position during stem and stance phase of each forelimb seems to be controlled by both sinus hair groups.

Other approaches try to examine if carpal sinus hairs can be used as sensors for substrate roughness or vibrations of the substrate. Therefore, the mechanical behavior of carpal sinus hairs is investigated during locomotion when they interact with different substrates. Due to the small size of carpal sinus hairs, this cannot be done during motion studies with living rats. Hence, these studies are done using a pedipulator, a mechanical gearing device which guides a dissected forelimb of a rat on a natural trajectory [21, 22].

5. MECHANICAL MODEL OF A VIBRISSA

From the engineering point of view the passive vibrissa in the first approximation is an Euler-Bernoulli beam. This model is applicable for understanding the basic principles of texture discrimination, see [42, 45]. We consider the vibrissa as a straight truncated conical beam (or a bending rod) of the length L initially fixed horizontally. The Cartesian coordinate system is placed such that the unperturbed axis of symmetry of the rod lies along the x axis and the origin is at the left cross-section, see Fig. 9. We assume that the vibrissa is pinned in the follicle and cannot experience deflection at the base $x = 0$. The vibrissa tip is pushed against an object, and so the end of the rod is also pinned at the right-hand support. The radius $r(x)$

of the vibrissa's circular cross-section evolves linearly along the axial direction: $r(x) = r_b + (r_t - r_b)\, x/L$, where r_b and r_t are respectively the radiuses at the base and the tip of the rod [30, 44].

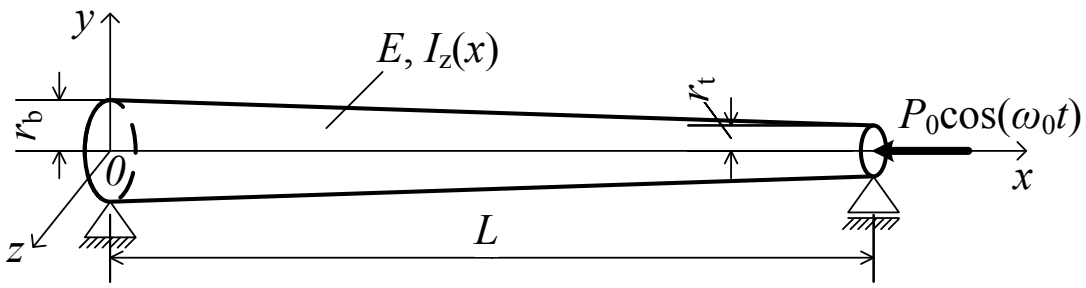

Fig. 9: Scheme of the mechanical model

As the vibrissa sweeps past an uneven surface, the roughness profile exerts a time-varying force at the tip of the vibrissa, causing it to oscillate at specific frequencies, see Fig. 9. In our model we assume that the periodic axial force $\vec{P}(t) = -P_0 \cos(\omega_0 t)\, \vec{\imath}$ is applied at the end of the rod $x = L$, where $\vec{\imath}$ is the unit vector of the x axis, see Fig. 9.

Consider small vibrations of the rod about its equilibrium configuration in the plane $x0y$. The motion of the rod under the applied concentrated harmonic force $\vec{P}(t)$ is described with a single partial differential equation of fourth order. With regard to the shear and the bending moments and in the absence a force of viscous damping, the equation of motion has the following form

$$\mathcal{L}(v) = m_0(x)\frac{\partial^2 v(x,t)}{\partial t^2} + \frac{\partial^2}{\partial x^2}\left(EI_z(x)\frac{\partial^2 v(x,t)}{\partial x^2}\right) + P_0\cos(\omega_0 t)\frac{\partial^2 v(x,t)}{\partial x^2} = 0, \quad (1)$$

where $v(x,t)$ is the transverse displacement of the axis points of the rod, $m_0(x) = \pi\rho r^2(x)$ is the mass per unit length, ρ is the mass density of the rod, E is Young's modulus, which is assumed to be constant along of the rod. Although it was shown experimentally that Young's modulus is larger near the vibrissa tip than near the base [33]. The moment of inertia of the cross-section $I_z(x)$ is defined as $I_z(x) = \pi r^4(x)/4$.

To solve Eq. 1 Galerkin's Method is used, that is a method for finding the approximate solution of a differential equation [23]. This powerful method allows to reduce a partial differential equation to an ordinary one. The basic idea of the method of Galerkin is the following. It is required to determine the solution of the equation $\mathcal{L}(v) = 0$, which satisfies boundary conditions. We shall seek an approximate solution of the equation in the form:

$$\tilde{v}(x,t) = \sum_{i=1}^{n} c_i \varphi_i(x) f_i(t),$$

where $\varphi_i(x), i = 1, \dots, n$, is a certain system of chosen basis functions satisfying the boundary conditions, and c_i are undetermined coefficients. Consider the functions $\varphi_i(x)$ to be linearly independent. In order that $\tilde{v}(x,t)$ be the solution of the equation $\mathcal{L}(v) = 0$, it is necessary that $\mathcal{L}(\tilde{v})$ be identically equal to zero. This requirement is equivalent to the condition of the orthogonality of $\mathcal{L}(\tilde{v})$ to all the functions of the system $\varphi_i(x), i = 1, \dots, n$. Stating these

conditions, the linear system of n equations for the determination of the coefficients c_i follows

$$\int_0^L \mathcal{L}\left(\sum_{i=1}^{n} c_i \varphi_i(x)\, f_i(t)\right)\varphi_i(x)dx = 0,\ \ i = 1, \dots, n.$$

Thus, substituting c_i in the expression for $\tilde{v}(x,t)$, the required approximate solution can be obtained.
In this paper, we assume a one-term approximation by Galerkin's Method of Eq. 1 in the form $\tilde{v}(x,t) = \sin(\pi x/L)\, f(t)$, which satisfies the pinned-pinned boundary condition of the rod:

$$v(0,t) = v(L,t) = 0,\quad \left.\frac{\partial^2 v(x,t)}{\partial x^2}\right|_{(0,t)} = \left.\frac{\partial^2 v(x,t)}{\partial x^2}\right|_{(L,t)} = 0.$$

Substituting this expression for $\tilde{v}(x,t)$ in Eq. 1, we obtain an ordinary differential equation written in dimensionless form as

$$\frac{d^2 f(\tau)}{d\tau^2} + [1 - \varepsilon\cos(\gamma\tau)]f(\tau) = 0. \qquad (2)$$

Here, dimensionless variables are introduces as follows:

$$\varepsilon = \frac{2\pi L^2}{a_1 E r_b^4} P_0,\ \ \gamma = \omega_0\sqrt{\frac{4a_0\rho L^4}{a_1 E r_b^2}},\ \ \tau = t\sqrt{\frac{a_1 E r_b^2}{4a_0\rho L^4}},\ \ \delta = \frac{r_t}{r_b}, 0 \le \delta \le 1,$$
$$a_0 = \frac{1}{6}(1+\delta+\delta^2) - \frac{1}{4\pi^2}(1-\delta)^2 > 0,$$
$$a_1 = \frac{\pi^4}{10}(1+\delta+\delta^2+\delta^3+\delta^4) - \frac{\pi^2}{2}(1-\delta)(1-\delta^3) + \frac{3}{4}(1-\delta)^4 > 0.$$

Parameters a_0 and a_1 of the Eq. 2 depend only on the ratio of the radiuses at the base and the tip of the rod $\delta = r_t/r_b$.

In particular, for the cylindrical rod with constant radius r_b, the moment of inertia of the cross-section is constant: $I_z(x) = \pi r_b^4(x)/4$. Hence, the approximate solution $\tilde{v}(x,t) = \sin(\pi x/L)\, f(t)$ is an exact one. In this case, Eq. 1 reduces to the same Eq. 2 with the parameters $a_0 = 1/2\,, a_1 = \pi^4/2$ as $\delta = 1$.

Eq. 2 is the second-order linear ordinary differential equation with periodic coefficient. The parameter ε depends on other biomechanical characteristics of the vibrissa and the amplitude of the applied force, and so it can be treated as a small parameter: $\varepsilon \ll 1$. Eq. 2 is known as Mathieu equation. Oscillations of the rod described by this equation are called parametrically excited. When the amplitude of oscillation caused by the periodic modulation of the force at the end of the rod increases steadily, the phenomenon of parametric resonance takes place. In parametric resonance, the rod performs oscillations whose amplitude progressively increases.

Periodic solutions of the Eq. 2 correspond to specific values of the dimensionless parameters ε and γ. If we put $\varepsilon = 0$ in Eq. 2, then it describes a simple harmonic motion with dimensionless natural frequency $\omega = 1$. It is shown that the parametric resonance takes place in the most intense way, when the value of the frequency γ is close to the doubled frequency of free vibrations of the rod [28]:

$$2 - \frac{\varepsilon}{2} < \gamma < 2 + \frac{\varepsilon}{2}. \tag{3}$$

This range of parameters ε and γ is called the region of the principal parametric resonance. The width of this region is proportional to the parameter ε. Parametric resonance can also take place at the frequency ranges close to the values of the form $2/n$ for any natural number n. However, the width of these resonance regions gets narrow proportionally to the value ε^n as n increases.

Thus, it is shown that the region of the principal parametric resonance depends on the biomechanical parameters of the vibrissa, such as the length, the radiuses at the base and the tip, the mass density and Young's modulus, see Eq. 3. For example, the arrangement by length of mystacial vibrissae on a mammal face may create a map of frequency sensitivity in the process of texture discrimination.

6. EXPERIMENTAL SETUP OF TECHNICAL VIBRISSA

To validate the results obtained by analytical investigations and numerical simulations, see [4, 5, 42, 45], an experimental setup is designed. The main idea of the experiment is to observe the interaction between an object and a technical vibrissa. That means that the reaction forces and moments should be measured for several object surface shapes and positions. The illustration of the experimental setup is presented in Fig. 10. Changing the real situation with an animal passing an object, we assume that the vibrissa with the measurement system stands still in the experiment, and the object is moved in a plane. Better dynamical and metrological conditions are the reason of this design principle.

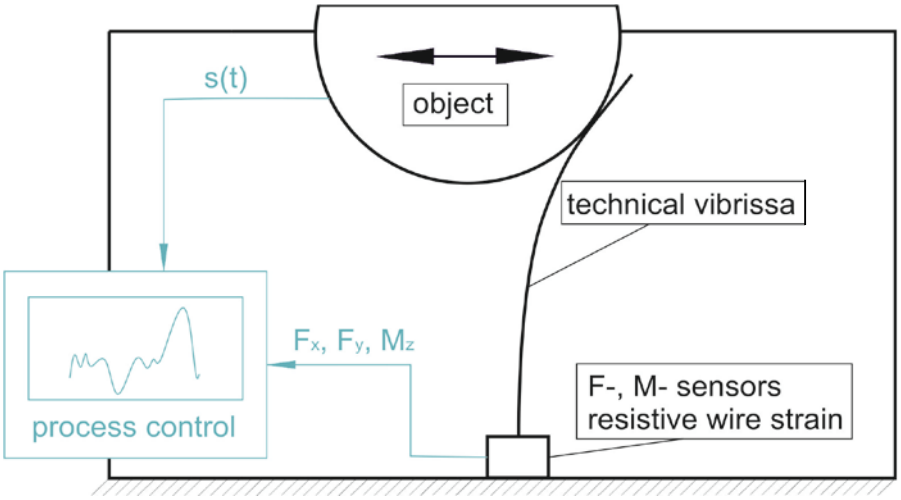

Fig. 10: Scheme of the experimental setup

The analytical models allow to calculate the forces and moment in the support of the vibrissa [45]. Using these reactions it is possible to reconstruct the surface shape of a touched object.

That is why the main task of the experiment is the estimation of the mentioned reactions with a high accuracy.

At first, the experimental setup consists of a technical vibrissa in macroscopic dimensions, that is the vibrissa is a steel beam with a length of about 300 mm. Even with the macroscopic model, the expected forces and moments are very small in sub-Newton and sub-Newton meter range, respectively. In the future investigations a miniaturization of the experimental setup is in the focus of the authors.

ACKNOWLEDGMENTS

This project is founded by DFG since 7/2013. Project name: „Technical non-visual characterization of substrate contact following the biological paragon of carpal vibrissae“ (Schm 1748/7-1, Wi 1664/4-1, Zi 540/16-1).

We want to thank Rommy Petersohn, John Nyakatura and Dirk Arnold for their assistance in the motion analysis. Thanks to the Chair of Micromechanic Systems, especially Martin Hoffmann, Lars Dittrich and Boris Goy for the opportunity to use of Keyence VW-9000. Institute for Bioprocessing and Analytical Measurement Techniques iba (Bad Heiligenstadt) provided access to SEM and EDX measurements. Max Planck Institute for Evolutionary Anthropology (Leipzig), especially Alexander Stößel supported the µCT-scans. The Center of Micro- and Nanotechnologies, especially Henry Romanus helped in FIB, EDX measurements and a lot more. And finally, we want to thank our students Marijke van den Berg, Susann Winkler, Susanne Mende, Caroline Fliegner, Sabine Wenzel, Monika Haase and Denise Recknagel for their interest and commitment to this “hairy topic”.

REFERENCES

[1] Andres, K. H.: Über die Feinstruktur der Rezeptoren an Sinushaaren. Zeitschrift für Zellforschung 75, 335 - 365 (1966)

[2] Arkley, K.; Grant, R. A.; Mitchinson, B.; Prescott, T. J.: Strategy change in vibrissal active sensing during rat locomotion. Current Biology 24 (13), 1507 - 1512 (2014)

[3] Beddard, F.: Observations upon carpal vibrissae in mammals. Proceedings of the Zoological Society London 72, 127 - 136 (1902)

[4] Behn C.: Mathematical modeling and control of biologically inspired uncertain motion systems with adaptive features. Habilitation Thesis Technische Universität Ilmenau (2013)

[5] Behn, C.; Will, C.; Steigenberger, J.: Unlike behavior of natural frequencies in bending beam vibrations with boundary damping in context of bio-inspired sensors. INTELLI 2014, The Third International Conference on Intelligent Systems and Applications, Seville, Spain, (2014)

[6] Carl, K.; Hild, W.; Mämpel, J.; Schilling, C.; Uhlig, R.; Witte, H.: Characterization of statical properties of rat’s whisker system. Sensors Journal, IEEE 12(2), 340 - 349 (2012)

[7] Carl, K.: Technische Biologie des Tasthaar-Sinnessystems als Gestaltungsgrundlage für tactile stiftführende Mechanosensoren. Berichte aus der Biomechatronik, Vol. 3, Universitätsverlag Ilmenau, Ilmenau (2009)

[8] Carvell, G. E.; Simons, D. J.: Biometric analyses of vibrissal tactile discrimination in the rat. Journal of Neuroscience 10, 2638 - 2648 (1990)

[9] Ebara, S.; Kumamoto, K.; Matsuura, T.; Mazurkiewicz, J. E.; Rice F. L.: Similarities and differences in the innervation of mystacial vibrissal follicle–sinus complexes in the rat and cat: a confocal microscopic study. Journal of Comparative Neurology 449, 103 - 119 (2002)

[10] Fischer, M. S.; Witte, H.: Legs evolved only at the end! Philosophical Transactions of the Royal Society A: Mathematical, Physical and Engineering Sciences, 365(1850), 185 - 198 (2007)

[11] Fundin, B. T.; Arvidsson, J.; Rice, F. L.: Innervation of nonmystacial vibrissae in the adult rat. The Journal of Comparative Neurology 357, 501 - 512 (1995)
[12] Gao, P.; Bermejo, R.; Zeigler, H.P.: Whisker deafferentation and rodent whisking patterns: behavioral evidence for a central pattern generator. The Journal of Neuroscience 21, 5374 - 5380 (2001)
[13] Garrett, S. B.: It's not you, it's me. Really. Nature Neuroscience 12, 374 - 375 (2009)
[14] Ginter, C. C.; Dewitt, T. J.; Fish, F. E.; Marshall, C. D.: Fused traditional and geometric morphometrics demonstrate pinniped whisker diversity. PLoS One 7, e34481 (2012)
[15] Gottschaldt, K.-M.; Iggo, A.; Young, D. W.: Functional characteristics if mechanoreceptors in sinus hair follicles of the cat. Journal of Physiology (London) 235, 287 - 315 (1973)
[16] Grant, R. A.; Mitchinson, B.; Fox, C. W.; Prescott, T. J.: Active touch sensing in the rat: anticipatory and regulatory control of whisker movements during surface exploration. Journal of Neurophysiology 101, 862 - 874 (2009)
[17] Grillner, S.; Zanger, P.: On the central generation of locomotion in the low spinal cat. Experimental Brain Research 34, 241 - 262 (1979)
[18] Halata, Z.: Sensory innervation of the hairy skin (light- and electronmicroscopic study). The Journal of Investigative Dermatology 101 (1), 75S - 81S (1993)
[19] Halata, Z.; Munger, B. L.: Sensory nerve endings in Rhesus monkey sinus hairs. The Journal of Comparative Neurology 192, 645 - 663 (1980)
[20] Hartmann, M. J.; Johnson, N. J.; Towal, R. B.; Assad, C.: Mechanical characteristics of rat vibrissae: resonant frequencies and damping in isolated whiskers and in the awake behaving animal. Journal of Neuroscience 23, 6510 - 6519 (2003)
[21] Helbig, T.; Voges, D.; Niederschuh, S.; Schmidt, M.; Witte, H.: Characterizing the substrate contact of carpal vibrissae of rats during locomotion. Proceedings of Living Machines (2014)
[22] Helbig, T.; Voges, D.; Niederschuh, S.; Schmidt, M.; Witte, H.: The mechanics of carpal vibrissae of *Rattus norvegicus* during substrate contact. Proceedings 58th IWK Ilmenau Scientific Colloquium (2014)
[23] Kantorovich, L.V; Krylov, V.I.: Approximate methods of higher analysis. Interscience Publ., New York (1958)
[24] Kastelein, R. A.; Van Gaalen, M. A.: The sensitivity of the vibrissae of a Pacific walrus (*Odobenus rosmarus divergens)* Part 1. Aquatic Mammals 14, 123 - 133 (1988)
[25] Kim, J.-N.; Koh, K.-S.; Lee, E.; Park, S.-C.; Song, W.-C.: The morphology of the rat vibrissal follicle-sinus complex revealed by three-dimensional computer-aided reconstruction. Cells Tissues Organs 193, 207 - 214 (2011)
[26] Klauer, G.: Vibrissen – Analyse eines Sinnesorgans. Habilitationsschrift, Universität Essen, Fachbereich Bio- und Geowissenschaften, Landschaftsarchitektur (1999)
[27] Krehbiel, M.: Anatomie der rostralen und caudalen Tasthaare beim Sambischen Riesengraumull (*Fukomys mechowii*) – Sinushaare oder Leithaare? Dissertationsschrift, Tierärztliche Hochschule Hannover, Hannover (2010)
[28] Landau, L.D.; Lifshitz, E.M.: Mechanics (Course of Theoretical Physics, Vol. 1), Pergamon Press, Oxford (1960)
[29] Lyne, A. G.: The systematic and adaptive significance of the vibrissae in the marsupialia. Proceedings of the Zoological Society of London 133, 79 - 133 (1959)
[30] Neimark, M. A.; Andermann, M. L.; Hopfield, J. J.; Moore, C. I.: Vibrissa resonance as a transduction mechanism for tactile encoding. Journal of Neuroscience 23, 6499 - 6509 (2003)
[31] Niederschuh, S. J.; Witte, H.; Schmidt, M.: The role of vibrissal sensing in forelimb position control during travelling locomotion in the rat (*Rattus norvegicus, Rodentia*). Journal of Zoology (in revision)
[32] Pocock, R. I.: On the facial vibrissae of mammalia. Proceedings of the Royal Society B: Biological Sciences 84 (3), 889 - 912 (1914)
[33] Quist, B.W.; Faruqi, R.A.; Hartmann M.J.: Variation in Young's modulus along the length of a rat vibrissa. - *J. Biomechanics*, vol. 44, pp. 2775-2781 (2011)
[34] Rice, F. L.: An attempt to find vibrissa-related barrels in the primary somatosensory cortex of the cat. Neuroscience Letters 53, 169 - 172 (1985)

[35] Rice, F. L.; Gomez, C.; Barstow, C.; Burnet, A.; Sands, P.: A comparative analysis of the development of the primary somatosensory cortex: interspecies similarities during barrel and laminar development. The Journal of Comparative Neurology 236, 477 - 495 (1985)
[36] Rice, F. L.; Kinnman, E.; Aldskogius, H.; Johansson, O.; Arvidsson, J.: The innervation of the mystacial pad of the rat as revealed by PGP 9.5 immunofluorescence. The Journal of Comparative Neurology 337 (3), 366 - 385 (1993)
[37] Rice, F. L.; Munger, B. L.: A comparative light microscopic analysis of the sensory innervation of the mystacial pad. II. The common fur between the vibrissae. The Journal of Comparative Neurology 252, 186 - 205 (1986)
[38] Rice, F.L.; Fundin, B. T.; Arvidsson, J.; Aldskogius, H.; Johansson O.: A comprehensive immunofluorescence and lectin binding analysis of vibrissal follicle sinus complex innervation in the mystacial pad of the rat. The Journal of Comparative Neurology 385, 149 - 184 (1997)
[39] Schmidberger, G.: Über die Bedeutung der Schnurrhaare bei Katzen. Zeitschrift für vergleichende Physiologie 17, 387 - 407 (1932)
[40] Shik, M. L.; Orlovsky, G. N.: Neurophysiology of locomotor automatism. Physiological Reviews, 56 (3), 465 - 501 (1976)
[41] Sokolov, V. E., Kulikov, V. E.: The structure and function of the vibrissal apparatus in some rodents. Mammalian Species 51(1), 125 - 138 (1987)
[42] Steigenberger J.: A continuum model of passive vibrissae, , Preprint No. M 13/32013, TU Ilmenau, Fakultät MN Ilmenau, Germany (2013)
[43] Vincent, S.B.: The tactile hair of the white rat. Journal of Comparative Neurology 23(1), 1 - 36 (1913)
[44] Voges, D.; Carl, K.; Klauer, G. J.; Uhlig, R.; Schilling, C.; Behn, C.; Witte, H.: Structural characterization of the whisker system of the rat. IEEE Sensors 12 (2), 332 - 339 (2012)
[45] Will, C.: Anwendung nichtlinearer Biegetheorie auf elastische Balken zur Objektabtastung am Beispiel passiver Vibrissen mit unterschiedlicher Lagerung, Master Thesis Technische Universität Ilmenau (2013)
[46] Yan, W.; Kan, Q.; Kergrene, K.; Kang, G.; Feng, X.; Rajan, R.: A truncated conical beam model for analysis of the vibration of the rat whiskers. Journal of Biomechanics 46, 1987 - 1995 (2013)

CONTACTS

Dipl.-Ing. T. Helbig thomas.helbig@tu-ilmenau.de

PD Dr. rer. nat. habil. M. Schmidt Schmidt.Manuela@uni-jena.de

Univ.-Prof. Dipl.-Ing. Dr. med. (habil.) H. Witte Hartmut.Witte@tu-ilmenau.de

Univ.-Prof. Dr.-Ing. habil. K. Zimmermann Klaus.Zimmermann@tu-ilmenau.de

